

# The influence of temperature on wave scattering of damaged segments within composite structures

Rilwan Kayode Apalowo<sup>1,\*</sup>, Dimitrios Chronopoulos<sup>1</sup>, and Muhammed Malik<sup>1</sup>

<sup>1</sup>Institute for Aerospace Technology & The Composites Group, The University of Nottingham, NG7 2RD, UK

**Abstract.** The increased use of composite materials in modern aerospace and automotive structures, and the broad range of launch vehicles' operating temperature imply a great temperature range for which the structures has to be frequently and thoroughly inspected. A thermal mechanical analysis is used to experimentally measure the temperature-dependent mechanical properties of a composite layered panel in the range of  $-100^{\circ}\text{C}$  to  $150^{\circ}\text{C}$ . A hybrid wave finite element/finite element computational scheme is developed to calculate the temperature-dependent wave propagation and interaction properties of a system of two structural waveguides connected through a coupling joint. Calculations are made using the measured thermomechanical properties. Temperature-dependent wave propagation constants of each structural waveguide are obtained by the wave finite element approach and then coupled to the fully finite element described coupling joint, on which damage is modelled, in order to calculate the scattering magnitudes of the waves interaction with damage across the coupling joint. The significance of the panel's glass transition range on the measured and calculated properties is emphasised. Numerical results are presented as illustration of the work.

## 1 Introduction

Aerospace and automotive structures operate within varying temperature range, which is typically between  $-100^{\circ}\text{C}$  to  $200^{\circ}\text{C}$  for launch vehicles and  $-60^{\circ}\text{C}$  to  $+50^{\circ}\text{C}$  for aircraft and automotive structures. On the other hand, aeronautics industries spend approximately 27% of an average modern aircraft's lifecycle cost on offline inspection and repair. Therefore, the temperature dependent non-destructive damage detection and evaluation is of paramount importance for monitoring the condition and residual life estimation of in-service aerospace structures.

The effect of high temperature on the thermomechanical response of various composite structures, such as multi-layered plates and shells [1], carbon plastic reinforced composite [2], fibre-reinforced plastic composite [3], glass epoxy composites [4] and carbon fibre epoxy composites [5], has been extensively assessed. However, investigation of the thermoacoustic behaviour of composites has been found almost in-existent in the open literature.

The numerical analysis of wave propagation within periodic structure is introduced in [6] and extended to formulate the wave finite element (WFE) method in [7]. The WFE has recently found application in predicting the vibroacoustic and dynamic properties of composite

\*e-mail: Rilwan.Apalowo@nottingham.ac.uk

panels and shells [8–12] with complex periodic structures [13, 14] having been investigated. The variability of vibroacoustic transmission through layered structures [16] and structural identification [17] have also been considered.

In this work, the temperature dependency of wave interaction with damage is exhibited using a FE-based computational scheme. The mechanical characteristics of a sandwich panel comprising carbon epoxy facesheets and a honeycomb core are experimentally measured using a Thermal Mechanical Analysis (TMA) configuration. In Sec. 2, the thermomechanical characteristics of the composite panel is presented. The WFE scheme for the calculation of wave interaction coefficients is presented in Sec. 3. In Sec.4 numerical results are presented. Conclusions are drawn in Sec.5.

## 2 Measurement of temperature dependent mechanical characteristics

The thermomechanical characteristics of a composite panel comprising of an orthotropic honeycomb core ( $E_x = E_y = 85$  MPa,  $G_{yz} = 44$  MPa,  $G_{xz} = 24$  MPa,  $\rho = 48$  kg/mm<sup>3</sup>,  $\nu_{xy}=0.23$ ) sandwiched between two carbon epoxy facesheets each consisting of four layers of 1-1 twilled weaves ( $E_x = E_y = 54$  GPa,  $G_{xy} = 8.5$  GPa,  $\rho = 1410$  kg/mm<sup>3</sup>,  $\nu_{xy}=0.09$ ) are experimentally measured on a TMA machine.

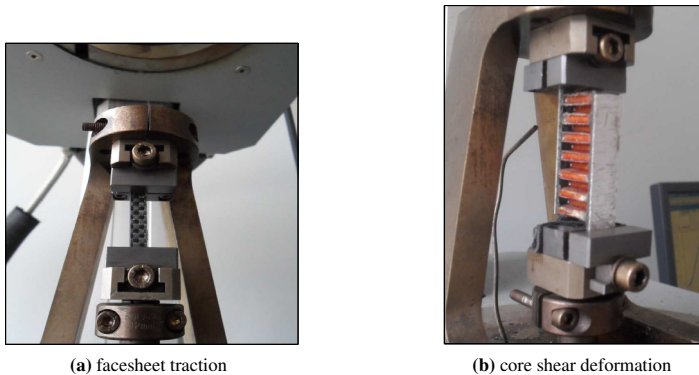
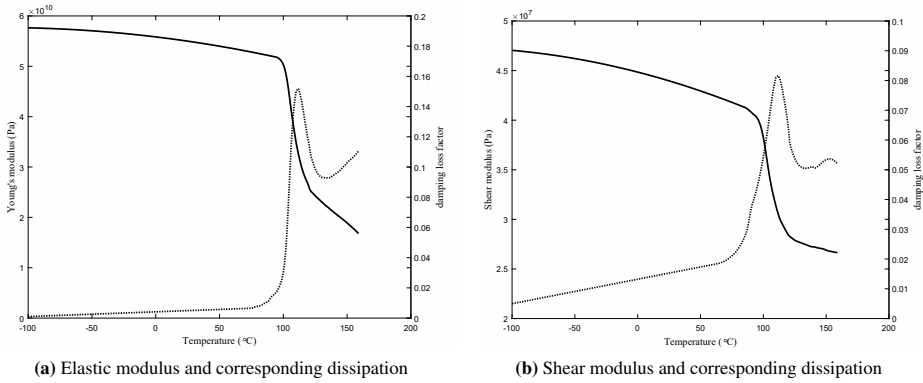


Figure 1. Configuration of a segment of the panel in the TMA machine

Temperature dependent elastic (of the facesheet) and shear (of the core) moduli are measured by subjecting a segment of the panel to longitudinal traction (Fig. 1a) and shear deformation (Fig. 1b) respectively. Respective material dissipation is measured using the phase lag (between stress and strain) determined as the ratio of loss modulus to the storage modulus. A constant 1 Hz excitation and a 0.1% deformation are imposed to the segment during the TMA measurements.

Measured elastic and shear moduli over a temperature range of  $-100^{\circ}\text{C}$  to  $160^{\circ}\text{C}$  are presented in Fig. 2. The moduli value decrease slightly while their corresponding material dissipation increase slightly with respect to temperature until  $90^{\circ}\text{C}$ . Thereafter, the resin included in the panel enters its glass transition temperature  $T_g$ . High peak is observed for dissipation in this range, while moduli decrease by about 45%. After the  $T_g$ , the moduli decrease with a steady rate while the dissipation after a short decrease starts increasing again due to the high viscosity of the melting resin.



**Figure 2.** Experimentally measured temperature dependent moduli (-) and corresponding dissipation (···) of the sandwich panel

### 3 Calculation of the temperature dependent elastic wave interaction by WFE scheme

Consider a system of two waveguides connected through a structural coupling joint (Fig. 3) which can contain exhibit complex mechanical behaviour such as damage, geometric or material linearities. Elastic wave interaction with inconsistencies along the joint is hereby calculated through a hybrid WFE-FE approach.

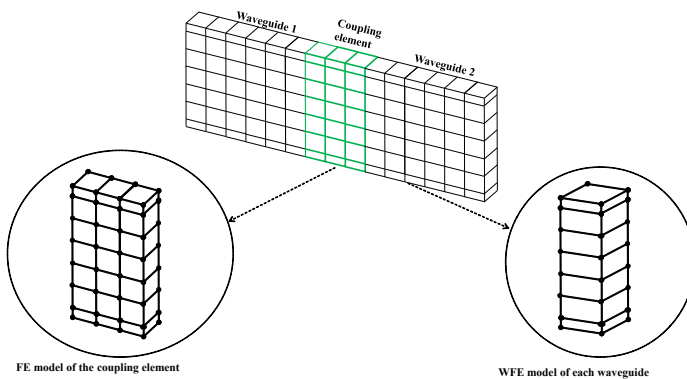


**Figure 3.** Caption of a system as two waveguides connected through a coupling joint

Elastic wave propagation along each arbitrarily layered waveguide is considered in the  $x$  direction. The frequency and temperature dependent Dynamic Stiffness Matrix (DSM) ( $\mathbf{D}(\omega, T) = \mathbf{K}(\omega, T) - \omega^2\mathbf{M}(\omega) + i\omega\mathbf{C}(\omega, T)$ ) of the waveguide's periodic segment can be partitioned with regards to its left and right sides, and internal DoFs. The WFE approach eliminates internal nodes by combining periodic segment theory with FE. Hence, the system is condensed to only left and right nodes DoFs with time harmonic behaviour expressed as

$$\begin{bmatrix} \mathbf{D}_{LL} & \mathbf{D}_{LR} \\ \mathbf{D}_{RL} & \mathbf{D}_{RR} \end{bmatrix} \begin{Bmatrix} \mathbf{q}_L \\ \mathbf{q}_R \end{Bmatrix} = \begin{Bmatrix} \mathbf{f}_L \\ \mathbf{f}_R \end{Bmatrix} \quad (1)$$

with  $\mathbf{q}$  and  $\mathbf{f}$  the displacement and forcing vectors respectively, and subscripts  $L$  and  $R$  the left and right nodal DoFs respectively.

Following the analysis presented in [17], the free wave propagation eigenproblem can be expressed as

$$\gamma \begin{Bmatrix} \mathbf{q}_L^{(s)} \\ \mathbf{f}_L^{(s)} \end{Bmatrix} = \mathbf{T} \begin{Bmatrix} \mathbf{q}_L^{(s)} \\ \mathbf{f}_L^{(s)} \end{Bmatrix} \quad (2)$$

whose eigenvalues and eigenvectors solution sets provide a comprehensive description of the propagation constants and the wave mode shapes for each of the elastic waves propagating in the structural waveguide at a specified frequency and temperature.

The wavemodes obtained through the WFE scheme, at each frequency and temperature, for each waveguide can be grouped into displacement and force components. Subsequently the modes can be concatenated as

$$\Psi_{\mathbf{q}}^{inc} = \begin{bmatrix} \Phi_{q1}^{inc} & \mathbf{0} \\ \mathbf{0} & \Phi_{q2}^{inc} \end{bmatrix} \quad (3)$$

with similar expressions for  $\Psi_{\mathbf{q}}^{ref}$ ,  $\Psi_{\mathbf{f}}^{inc}$  and  $\Psi_{\mathbf{f}}^{ref}$ . *inc* and *ref* denote the positive and negative going waves respectively, and 1, 2 the waveguides indices. Assume modal decomposition, the physical domain can be converted to the wave domain as

$$\begin{Bmatrix} \mathbf{q}_L \\ \mathbf{f}_L \end{Bmatrix} = \Phi \begin{Bmatrix} \mathbf{Q}^{inc} \\ \mathbf{Q}^{ref} \end{Bmatrix} \quad (4)$$

where  $\mathbf{Q}$  denotes the amplitudes of the wave modes.

The coupling joint is modelled using full FE approach. Its DSM can be partitioned into interface (with the waveguides) and non-interface nodes DoFs. Condensing the non-interface DoFs, the DSM can be expressed as

$$\mathbf{D}_C^* = \mathbf{D}_{ii} - \mathbf{D}_{in} \mathbf{D}_{nn}^{-1} \mathbf{D}_{ni} \quad (5)$$

where subscript  $i$  corresponds to the interface DoFs and  $n$  the non-interface DoFs. Applying displacement continuity and equilibrium of forces at the connecting interfaces, the scattering matrix  $\mathbf{S}$  of the joint, whose partitions relate the amplitudes of the incident and scattered waves, can be expressed as

$$\begin{Bmatrix} \mathbf{Q}_1^{ref} \\ \mathbf{Q}_2^{ref} \end{Bmatrix} = \mathbf{S} \begin{Bmatrix} \mathbf{Q}_1^{inc} \\ \mathbf{Q}_2^{inc} \end{Bmatrix} \quad (6)$$

where

$$\mathbf{S} = -[\Psi_{\mathbf{f}}^{ref} - \mathbf{D}_C^* \Psi_{\mathbf{q}}^{ref}]^{-1} [\Psi_{\mathbf{f}}^{inc} - \mathbf{D}_C^* \Psi_{\mathbf{q}}^{inc}] \quad (7)$$

with diagonal elements being the reflection coefficients and off diagonal the transmission coefficients of the waves.

## 4 Numerical case study

The computational scheme exhibited above is applied on the numerical computation of the wave scattering coefficients of damaged segment in the sandwich panel over temperature range -100°C to 150°C.

The asymmetric layered sandwich panel, with thermomechanical properties as presented in Sec. 2, comprises of upper and lower facesheets and core having a cross section of 15.7

$mm \times 8 mm$  and thicknesses of  $2 mm$ ,  $1 mm$  and  $12.7 mm$  respectively. Wave interaction coefficient at the coupling joint on which a crack of depth index 0.4 (fraction of the plate thickness) is modelled. The crack is located at  $1 mm$  along the  $x$  direction of the coupling joint.

Three propagating wave types are obtained up to frequency of  $110 kHz$ . In practice, the modes of each wave can be excited in a full FE transient simulation in which the WFE computed wave modes is applied as time-dependent harmonic displacement at the left end of the panel. A 10 cycle Hanning window modulated tone burst signal is used for all transient excitation.

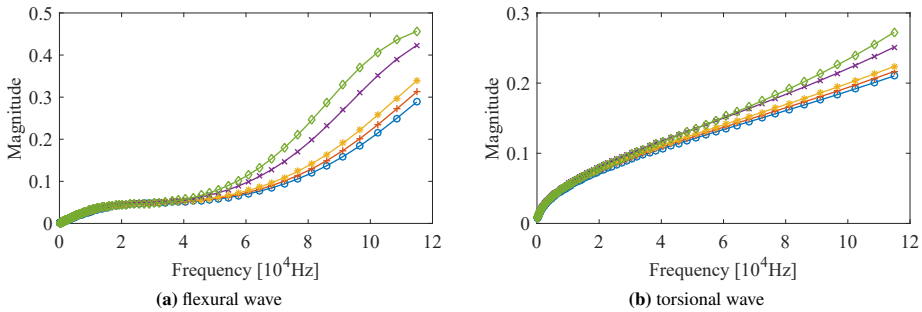


**Figure 4.** Temperature dependent reflection coefficient magnitude for the panel at  $-100^{\circ}C$  (o),  $25^{\circ}C$  (+),  $90^{\circ}C$  (\*),  $110^{\circ}C$  (x) and  $150^{\circ}C$  (◊)

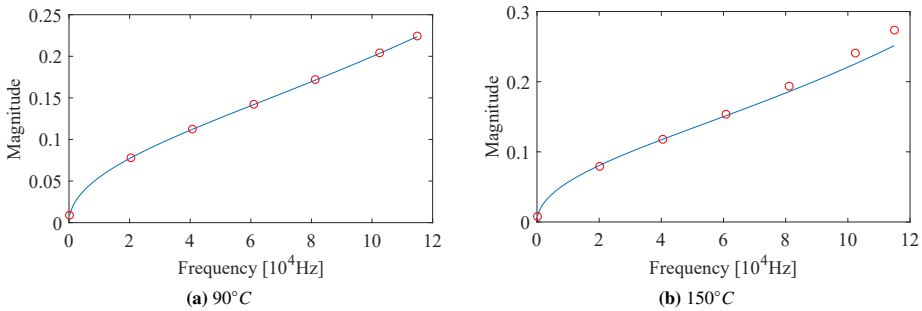


**Figure 5.** Reflection coefficient magnitude of the axial wave along the panel just before ( $90^{\circ}C$ ) and after ( $150^{\circ}C$ ) the glass transition region: current scheme (-), full transient calculation (o)

Excellent agreement is observed between the axial wave reflection results obtained through the presented approach and through the full FE transient response prediction as shown in Fig. 5. Moreover, the effect of temperature on the reflection coefficient in the temperature range below, within and after the glass transition temperature varies significantly (Fig. 4). Below the glass transition temperature, there exist slight increase in the reflection coefficients of all the wave types with a maximum difference of about 10% per  $50^{\circ}C$  change in temperature. Above the glass transition temperature, a considerable difference is observed with respect to temperature change with an observed difference of about 28% per  $50^{\circ}C$  change in temperature.

## 5 Conclusion

A FE-based computational model was presented for calculating reflection and transmission coefficients from wave interaction with structural damage. The impact of temperature dependent mechanical characteristics of a layered sandwich structure on the interaction coefficients is also exhibited. Results exhibited a large difference between the moduli and the material dissipation values at and above the glass transition region of the panel resin. Similar behaviour is observed in the wave interaction results. It can be concluded that temperature is a significant factor that should be taken into consideration in the design process of aerospace structure.

## References

- [1] A.K. Noor, U.S. Burton, *Appl Mech Rev.*, 45(10), 419–446, (1992).
- [2] L.B. Rozenberg, L.E. Grishchak, V.M. Ilman, *Polymer Mechanics*, 7, 320–322, (1973).
- [3] M.R. Maheri, R.D. Adams, J.M. Galtonde, *Composites, Science and Technology*, 56, 1425–1434, (1996).
- [4] Y.J. Dimitrienko, 28, 453–461, (1997).
- [5] O. Putkis, R.P. Dalton, A.J. Croxford, *Ultrasonic*, 60, 109–116, (2015).
- [6] D.J. Mead, *Journal of Sound and Vibration*, 27(2), 235–260, (1973).
- [7] B.R. Mace, D. Duhamel, M.J. Brennan, L. Hinke, *The Journal of the Acoustical Society of America*, 117(5), 2835–2843, (2005).
- [8] D. Chronopoulos, B. Troclet, M. Ichchou, J.P. Laine, *Composites Part B: Engineering*, 43(4), 1837–1846, (2012).
- [9] D. Chronopoulos, B. Troclet, O. Bareille, M. Ichchou, 96, 111–120, (2013).
- [10] D. Chronopoulos, M. Ichchou, B. Troclet, O. Bareille, *Composite Structures*, 97, 401–404, (2013).
- [11] Chronopoulos, D., Ichchou, M., Troclet, B. and Bareille, O. *Applied Acoustics*, 74(12), 1394–1405, (2013).
- [12] D. Chronopoulos, M. Ichchou, B. Troclet, O. Bareille, *Aerospace Science and Technology*, 30, 192–199, (2013).
- [13] D. Chronopoulos, M. Collet, M. Ichchou, *Materials*, 8(2), 815–828, (2015).
- [14] D. Chronopoulos, I. Antoniadis, M. Collet, M. Ichchou, *Wave Motion*, 58, 165–179, (2015).
- [15] J.F. Doyle, *Wave Propagation in Structures: Spectral Analysis Using Fast Discrete Fourier Transforms* (Springer, 1997).
- [16] R.K. Apalowo, D. Chronopoulos, M. Ichchou, Y. Essa, F.M. De-La-Escalera, *Proceedings of the Institution of Mechanical Engineers, Part C: Journal of Mechanical Engineering Science*, 231, 3042–3056, (2017).
- [17] D. Chronopoulos, C. Droz, R.K. Apalowo, M. Ichchou, W.J. Yan, 182, 566–578, (2017).